CHEMICAL BATH DEPOSITION OF Ti-DOPED ZnO NANORODS FOR UV-PHOTODETECTOR APPLICATIONS

SHAKER ALI HAMAD ABU BIDIER

UNIVERSITI SAINS MALAYSIA

2018

CHEMICAL BATH DEPOSITION OF Ti-DOPED ZnO NANORODS FOR UV-PHOTODETECTOR APPLICATIONS

by

SHAKER ALI HAMAD ABU BIDIER

Thesis submitted in fulfillment of the requirements
for the degree of
Doctor of Philosophy

April 2018

ACKNOWLEDGMENT

In the name of Allah, the beneficent the merciful.

Alhamdulillah, all thanks to The Almighty with His grace, I managed to complete this thesis successfully. Firstly, I would like to express my most profound gratitude to my supervisor, Professor Dr. Md Roslan Hashim, for the continuous support of my Ph.D. study and related research, for his gaudiness, clever comments, and suggestions. He taught me how to be a good researcher. I thank him a lot, and I hope to Allah that he gives him the good health and the long age.

I acknowledge the Universiti Sains Malaysia (USM) for its financial support to do this research. I would like to thank the technical staff in the nano-optoelectronics research laboratory and the solid-state physics laboratory all, and my friends and colleagues at the school of physics for their co-operation, and technical assistance.

My special thanks to my dear family; my dear father, my dear mother, and my brothers: Alla, Amer, Yazed, Izzdieen, Ja'afer, and Ahmad, also my sisters Ola, and Ayat, and their families, for their great love, prayers, and encouragement.

My heartfelt grates to my beloved wife; Islam Mohammad Alomari, for her long-patient, great love, and endless supporting me during this important time. Without her, I could not have a chance to complete this study. I thank her family also, her father, her mother, and her brothers and sisters, especially; Weal, and Bilal and their families, for their important support, prayers, and patients.

Shaker Ali Hamad Abu Bidier

Penang, Malaysia, April 2018

TABLE OF CONTENTS

LIST OF TABLES

LIST OF FIGURES

LIST OF SYMBOLS

D	Average crystallite size
G	Current gain
I_d	Dark current
θ	Diffraction angle
$e–h$	electron–hole
E_g	Energy band gap
E_F	Fermi level
β	Full width at half maximum
$E_1(H)$	High-Raman mode
P	Incident optical power
a, c	Lattice constants
$E_2(L)$	Low-Raman mode
Φ_m	Metal work function
$\Phi_{m.s}$	Metal-semiconductor contact
O_i	Oxygen interstitial
V_o	Oxygen vacancy
I_{ph}	Photocurrent
A_1, B_1, E_1	Raman modes
R	Responsivity
Θ_B	Schottky barrier height
χ_o	Semiconductor electron affinity
$E_{F.S}$	Semiconductor Fermi level
Φ_s	Semiconductor work function
S	Sensitivity
e_{zz}	Strain
c_o	Unstrained lattice constant
E_o	Vacuum energy
λ	Wavelength
Zn_i	Zinc interstitial

LIST OF ABBREVIATIONS

a.u	Arbitrary unit
BM	Burstein Moss effect
CB	Conduction band
CBD	Chemical bath deposition
DI	Deionized water
DLE	Deep-level emission
EDX	Energy dispersive X-ray spectroscopy
EF-TEM	Energy-filtered transmission electron microscopy
FESEM	Field emission scanning electron microscopy
FTIR	Fourier-transform infrared spectroscopy
FTO	F-doped SnO_2
FWHM	Full width at half maximum
MSM	Metal-Semiconductor-Metal
NBE	Near-band edge emission
NRs	Nanorods
NSs	Nanostructures
PD	Photodetector
PL	Photoluminescence
RF	Radio frequency
sccm	Standard cubic centimeters per minute
TZ	Ti-doped ZnO
UV	Ultraviolet
VB	Valance band
XRD	X-ray diffraction

ENDAPAN MANDIAN KIMIA BAGI NANOROD ZnO TERDOP Ti UNTUK APLIKASI PENGESAN FOTO UV

ABSTRAK

Kajian ini menerangkan tentang pengaruh titanium (Ti) kepada ciri nanorod zink oksida (ZnO) yang dihasilkan di atas substrat Si dengan menggunakan kaedah pemendapan mandian kimia dengan titanium oksida (TiO_2) sebagai sumber Ti. Hasil belauan sinar-X (XRD) menunjukkan peningkatan saiz hablur dari 44.4 nm di dalam sampel yang tidak terdop kepada 51.2 nm di dalam sampel yang telah terdop. Hasil kefotopendarcahayaan telah menunjukkan peningkatan jurang tenaga dari 3.241 eV bagi sampel yang tidak terdop kepada 3.293 eV bagi sampel yang telah terdop. Ukuran kesan Hall juga telah menunjukkan peningkatan dari segi ciri elektrikal bagi sampel terdop, di mana kepekatan pengangkut telah meningkat dari 8.7×10^{16} cm^{-3} untuk sampel yang tidak terdop kepada 2.1×10^{18} cm^{-3} untuk sampel terdop. Kesan masa pertumbuhan ke atas morfologi dan ciri struktur ZnO yang terdop dengan Ti telah dikaji. Dengan pemanjangan tempoh pertumbuhan, imej mikroskop penghantaran elektron telah menunjukkan kesan hakisan ke atas nanorod secara. Hal ini boleh dikaitkan dengan reaksi pelarutan ZnO dengan peningkatan masa pertumbuhan, cth 6.5 jam. Hasil ini menunjukkan peranan masa pertumbuhan di dalam pengubahsuaian arah pertumbuhan. Akhirnya, nanorod ZnO yang telah terdop dengan Ti telah dibangunkan menjadi peranti logam-semikonduktor-logam. Ciri fotoelektrik telah ditingkatkan di dalam peranti bagi ZnO terdop dengan Ti berbanding peranti ZnO yang tidak terdop. Bagi peranti yang tidak terdop, arus foto, kefotosensitifan, dan kesambutanan masing-masing adalah 61 μA, 1151 %, dan 37.4 mA/W. Walaubagaimanapun, bagi peranti yang telah terdop, ciri masing-masing ini telah ditingkatkan kepada 340 μA, 2518 %, dan 217.9 mA/W. Peningkatan ini

menunjukkan berlakunya pengubahsuaian yang baik di dalam ciri struktur, optikal, dan elektrikal disebabkan penambahan Ti di dalam struktur kekisi ZnO. Hasil yang telah diperolehi menunjukkan bahawa nanorod ZnO terdop dengan Ti menggunakan pemendapan mandian kimia adalah sesuai untuk aplikasi optoelektronik.

CHEMICAL BATH DEPOSITION OF Ti-DOPED ZnO NANORODS FOR UV-PHOTODETECTOR APPLICATIONS

ABSTRACT

This work studied the effects of titanium (Ti) on the properties of zinc oxide (ZnO) nanorods (NRs) grown on Si substrates using chemical bath deposition method with TiO_2 as a Ti source. X-ray diffraction (XRD) results showed an increase in the crystallite size from 44.4 nm in the undoped sample to 51.2 nm in the doped sample. Photoluminescence results revealed an increment in the energy band gap from 3.241 eV for the undoped sample to 3.293 eV for the doped sample. Hall effect measurements also showed an enhancement in the electrical properties of doped samples, the carrier concentration increased from 8.7×10^{16} cm^{-3} for the undoped sample to 2.1×10^{18} cm^{-3} for the doped sample. The effects of growth time on the morphology and structure properties of Ti-doped ZnO were studied. With prolong the growth time; energy-filtered transmission electron microscopy images revealed an erosion on the lateral of NRs. This could attribute to the dissolution reaction of ZnO for longer growth time i.e. 6.5h. These results display the role of growth time in the modification of the growth directions. Finally, Ti-doped ZnO NRs based on metal-semiconductor-metal was fabricated. The photoelectric parameters were enhanced for Ti-doped ZnO device as compared to that of the undoped ZnO device. For the undoped device the photocurrent, photosensitivity, and responsivity were 61 μA, 1151 %, and 37.4 mA/W, respectively. However, for the doped device, the parameters were enhanced to 340 μA, 2518 %, and 217.9 mA/W, respectively. This enhancement indicated an improvement in the structural, optical and electrical properties due to the incorporation of Ti into the ZnO lattice structure. The obtained

results demonstrate that the Ti-doped ZnO NRs prepared using chemical bath deposition is suitable for optoelectronic applications.

CHAPTER 1: INTRODUCTION

1.1 Introduction

Introducing impurities into an intrinsic semiconductor was described to be a useful method for improving its fundamental properties; this process is called doping [1]. Zinc oxide (ZnO) is considered as a suitable host semiconductor that can receive dopant impurities [2]. This refers to its promising properties such as direct wide band gap (3.37 eV) and large binding energy (60 meV) at room temperature. In addition, ZnO has several advantages such as low cost, environmentally-friendly, biocompatibility, thermal and chemical stability, as well as high transmittance in the visible spectrum [3-5].

ZnO has found various potential applications like solar cells, gas sensors, light-emitting diodes, ultraviolet (UV) -photodetectors and other optical applications [6, 7]. The performance of these applications depends on its properties; therefore, by doping, it can modify these properties and then improve their performance. Various researchers studied the effectiveness of doping on the properties of ZnO including structural, electrical, and optical properties [8-10].

ZnO nanostructures (NSs) have been doped using different elements and methods such as Cu-doped ZnO fabricated using the sol-gel method [11], Al-doped ZnO prepared using the hydrothermal method [12], Mg-doped ZnO synthesised using the atomic layer deposition technique [13], and Ag-doped ZnO grown by radio frequency (RF) magnetron sputtering [14]. In addition, Ti is a suitable element that can be used to dope ZnO lattice structure without any change in the original structure due to the small ionic size of Ti^{+4}, which is 0.068 nm, smaller than Zn^{+2} (0.074 nm). Therefore, Ti^{+4} can easily substitute Zn^{+2} sites within the ZnO crystal lattice [15].

Moreover, Ti has a massive balance electrons of (4) more than that of Zn (2), which increases the carrier concentration and then enhance the electrical properties such as conductivity [16, 17].

Doping is essential to enhance the properties of a common semiconductor such as ZnO for various applications like metal-semiconductor-metal (MSM) UV-photodetectors (PDs). Though, their performance depends on the properties of semiconductor that are used to fabricate PDs. Previously, PDs based on doped-ZnO films showed better performance than the undoped-ZnO [7, 18, 19].

This work aims to synthesize and characterize Ti-doped ZnO nanorods (NRs) using the chemical bath deposition (CBD) technique for potential UV applications. Ti-doped-ZnO NRs demonstrated interesting effects on the properties of ZnO that may offer further research works and other potential applications.

1.2 Problem statement

Many physical methods were used to prepare Ti-doped ZnO using titanium oxide (TiO_2). These methods include RF sputtering [16], atomic laser deposition [20], solid state reaction [21] and pulsed laser deposition [22]. These methods are costly and need high-temperature and high vacuum ambient, especially when compared to CBD method, which is low in cost, simple procedures and low-operation-temperature [23]. In chemical methods, TiO_2 has not been used to prepare Ti-doped ZnO due to its' non-volatile nature [24]. Ti sources that commonly used are titanyl acetylacetonate ($TiC_{10}H_{14}O_5$) [25], titanium (IV) butoxide ($C_{16}H_{36}O_4Ti$) [26-28], titanium (IV) isopropoxide ($C_{12}H_{28}O_4Ti$) [29, 30], and ammonium hexafluorotitanate ($(NH_4)_2TiF_6$) [31]. It can be noticed that those researchers used

complicated Ti sources. In this work, TiO_2 as a simple Ti source was used to synthesis Ti-doped ZnO using CBD method.

TiO_2 is a non-volatile component [24]. In order to break the chemical bonds an ultrasonic treatment that generates extraordinary conditions such as high temperatures (even reaching to 5000 K) and high pressure (about 1000 atm) was used [32-34].

Ti^{+4} can easily substitute Zn^{+2} site in the ZnO lattice structure due to its' smaller ionic size [15]. In this study, the properties of Ti-doped ZnO sample showed an enhancement as compared to the undoped sample. This enhancement refers to the simple Ti source and pre-treatment procedures that ease the incorporation process into the proper sites, (sites of Zn^{+2}), in ZnO. However, the results of this study are in contrast with previous results that used different Ti sources [30, 31, 35]

In CBD, the growth time is an important factor that can control the properties of ZnO NSs. By increasing the growth time; more Zn^{+2} and O^{-2} may assemble into the ZnO lattice, which modifies the structural and the morphological properties of ZnO [36-38]. In this study, the effects of growth time on the properties of Ti-doped ZnO were investigated. MSM-UV-PDs were fabricated using Ti-doped ZnO NRs. The effects of Ti on photoelectrical enhancement parameters of UV PDs were discussed.

1.3 Objectives of this study

The main objectives of the current study are:

1. To synthesis Ti-doped ZnO NRs on silicon substrates using CBD method and TiO_2 as a Ti source.

2. To study the effects of growth time on morphological and structural properties of Ti-doped ZnO NRs.
3. To investigate the effects of Ti dopant on the characterizations of ZnO-MSM-UV-PDs.

1.4 Originality of this study

The originality of this study involves the following aspects:

1. Synthesis of Ti-doped ZnO NRs using CBD method with TiO_2 as a Ti dopant source for the first time.
2. Investigation the effects of growth time on the erosion phenomena at surface of Ti-doped ZnO NRs that prepared using CBD method with TiO_2 as a Ti dopant source for the first time.
3. Fabrication of fast response MSM-UV-PDs based on Ti-doped ZnO NRs that prepared using CBD method and TiO_2 as a Ti dopant source for the first time.

1.5 Scope of this study

In this work, undoped and Ti-doped ZnO NRs have been grown using CBD method with TiO_2 as a Ti source on a silicon substrate. ZnO NRs have been prepared at different precursor concentrations to determine the optimum concentration. The best ZnO synthesis concentration was used to prepare Ti-doped ZnO. The effects of Ti incorporation on ZnO properties were studied. The effects of deposition time on Ti-doped time were characterised. The undoped and Ti-doped ZnO samples were applied in the fabrication of MSM UV-PDs.

1.6 Outline of the thesis

This thesis consists of six chapters. Chapter 1 presents a brief introduction to the current study, the problem statement, objectives of the research, scope of the study and thesis originality. Chapter 2 discusses the fundamental properties of ZnO semiconductor, and the mechanism of CBD technique that used to grow ZnO NSs. An introduction to doping in semiconductors, including the definition, types and effects, were described. The fundamental knowledge and experimental study on Ti-doped ZnO were reviewed. Theoretical concepts belonging to MSM photodetector were introduced. Chapter 3 describes the methodology and the experimental features used in this study. Chapter 4 presents the results and discussions of synthesis and characterisation of undoped and Ti-doped ZnO NRs using the CBD method on silicon substrates. Then, the MSM photodetectors using the undoped and Ti-doped ZnO NRs were fabricated and characterised. Chapter 5 investigates the effects of the growth time on the structural and morphological properties of Ti-doped ZnO; next, MSM-photodetectors were fabricated and characterised. Finally, the conclusions of this study and recommendations for future works are presented in Chapter 6.

CHAPTER 2: LITERATURE REVIEW

2.1 Introduction

This chapter describes the fundamental properties of the ZnO semiconductor. The mechanism of CBD method is discussed. Previous works on Ti-doped ZnO NSs and ZnO NSs prepared using CBD were also reported. The effects of doping on physical properties of semiconductors and their importance are briefly explained.. Finally, the basic concepts of the MSM UV-PDs are described.

2.2 Background of ZnO

ZnO is an important n-type semiconductor with a direct band gap of 3.37 eV and large exciton energy of 60 meV at room temperature [5]. ZnO has been used in numerous areas such as solar cells technology, gas sensors, light-emitting diodes and UV-photodetection applications [38, 39]. ZnO has three phases (see Figure 2.1), the hexagonal-wurtzite structure is the most thermodynamically stable phase in normal conditions. In this phase, every Zn cation is surrounded by 4 oxygen anions and vice versa. This structure has two lattice parameters of *a* and *c*. Table 2.1 summarises the physical properties of ZnO. .

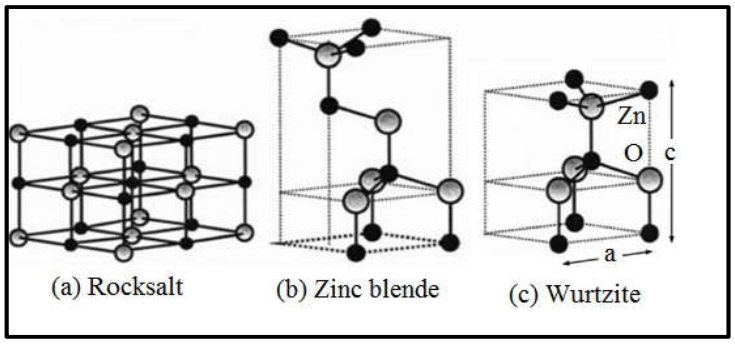

Figure 2-1 ZnO semiconductor phases [40].

Table 2-1 Physical properties of ZnO semiconductor at 300 K [41].

Property	**Value**
Lattice parameters (*a*, *c*)	0.32495 nm, 0.52069 nm
Energy ban gap	3.37 eV
Density	5.606 g/ cm^3
Refractive index	2.008
Dielectric constant	8.66
Intrinsic carrier concentration (cm^{-3})	~10^6 cm^{-3}
Melting point	1975 ^oC

ZnO NSs has various types of intrinsic defects such as vacancies and interstitials [42]; these defects strongly effect the properties of ZnO. The photoluminescence (PL) system is a non-destructive technique that is widely used to study the optical properties of the ZnO semiconductor [43, 44]. The typical PL spectrum of ZnO possesses two peaks (see Figure 2.2), one in UV emission around (370-400 nm) called the near band edge (NBE), and another in the visible region in the range of (450-700 nm) called the deep level emission (DLE) [45]. NBE is attributed to the recombination of free excitons in the exciton-exciton collision [46], this emission is a key factor of ZnO in optoelectronic devices such as UV-photodetectors [47, 48]. The DLE is referred to the photo-generated electrons trapped by deep defects within the band gap [42]. The optical quality (NBE/DLE) is an important factor that indicates favourable optical and structural properties; high optical quality indicates good film quality [49].

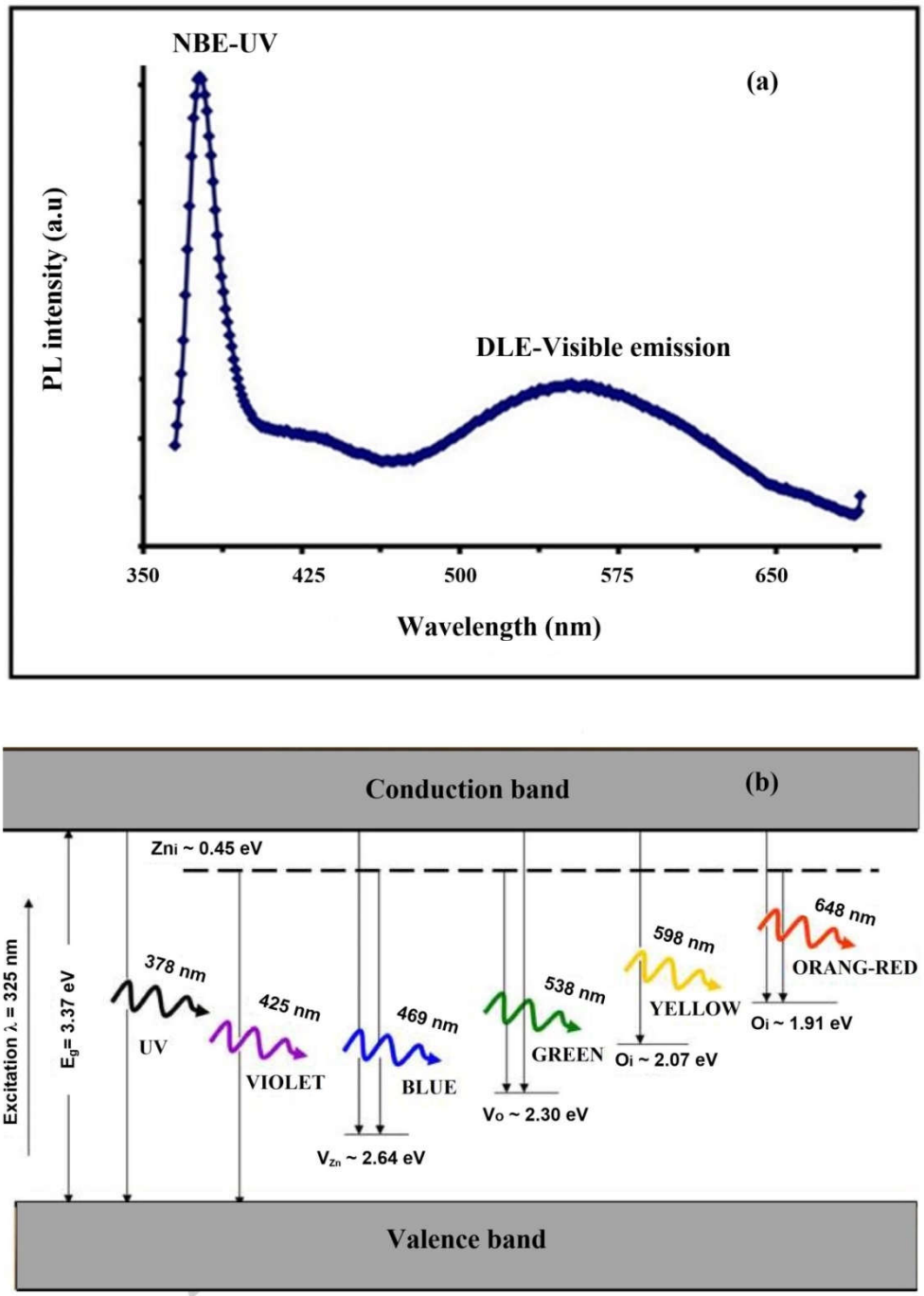

Figure 2-2 (a) Typical PL spectrum of ZnO NSs [50], (b) schematic diagram shows the energy levels of defects in ZnO [51].

2.3 Chemical growth techniques of ZnO NSs

ZnO NSs have been grown using several chemical methods such as sol-gel method, hydrothermal method, and CBD. The sol-gel method is a chemical technique used to prepare thin films. In this method, a precursor solution is prepared,

and then converted to sol-gel that is used to coat a substrate using spin-coating or dip-coating. The substrate is then heated to evaporate the solvent and finally, annealed to produce the crystallized structure. However, this method has the disadvantage of low film quality, less uniform in surface morphology and cracks [52, 53].

In a hydrothermal method, the ZnO deposition reaction is carried out in a steel container called an autoclave [54, 55]. The autoclave container is costly, and this represents the main limitation of this method [56]. Comparatively, the CBD method is simple to use than hydrothermal and sol-gel methods. In this method, glassware can be used to grow NSs [37, 57, 58]. Also, CBD has several advantages such as low cost, simple procedures and low-temperature technique in the range of 65-95 ^{o}C [23, 58]. Moreover, CBD has been used to synthesise various types of ZnO NSs such as NRs, nanowires, nano-cones, nanoparticles and nanotubes [59-61]. Additionally, CBD is a good method to synthesise NSs on a wide substrate that could be useful for some industrial applications [62]. Furthermore, in CBD method, various parameters such as deposition temperature, time, pH, substrate types and precursor concentration are used to control the properties of the as-grown structures [63, 64]. Doping structures can also be synthesised using CBD where various materials are introduced into the deposition pot [10, 12].

Generally, to synthesise ZnO NSs using CBD, two basic materials are needed: Zn source and O source. Many research groups had employed $Zn(NO_3)_2.6H_2O$ as a source of Zn while hexamethylenetetramine (HMTM, $C_6H_{12}N_4$) was used to produce OH^{-1} group ion via reaction with a water molecule. Production OH^{-1} group occurs via two steps, the first one: HMTM reacts with water (H_2O) and produces NH_3. The second: NH_3 also reacts with water molecules to produce OH^{-1}

group ions. OH^{-1} combines with Zn^{+2} to produce $Zn(OH)_2$ and ZnO molecules, which represents the basic unit to form the ZnO NSs [62, 65]. The concentration of $Zn(NO_3)_2.6H_2O$ and HMTM plays a significant role in controlling the properties of the as-grown structure. The properties of ZnO NSs can be controlled by adjusting the solution concentration in the first step of the deposition reaction [23].

In CBD method, the mechanism of ZnO synthesis can be described in the following equations (2.1-2.5) [6]. The first and second equations represent the reaction of HMTM with H_2O to make a basic environment via the generation of OH^{-1} ions. The OH^{-1} ions react with the Zn^{+2} ions to produce $Zn(OH)_2$. Finally, $Zn(OH)_2$ is dehydrated to produce ZnO. It is important to refer that the temperature of reaction plays an important role in decomposing the $Zn(OH)_2$ to form ZnO [5, 66].

$$C_6H_{12}N_4 + 6H_2O \rightarrow 6HCHO + 4NH_3 \quad (2.1)$$

$$NH_3 + H_2O \rightarrow NH_4^+ + OH^- \quad (2.2)$$

$$Zn(NO_3)_2 \rightarrow Zn^{+2} + 2NO_3^- \quad (2.3)$$

$$Zn^{+2} + 2OH^- \rightarrow Zn(OH)_2 \quad (2.4)$$

$$Zn(OH)_2 \xrightarrow{\Delta} ZnO + H_2O \quad (2.5)$$

2.4 ZnO prepared using CBD

Li et al. [23] investigated the effects of growth parameters (such as precursor concentration, growth time and temperature) on the morphology of ZnO NRs prepared by CBD method on silicon substrates. They found that the morphological parameters, including the average diameter and length, strongly responded to growth parameters. Increase the precursor concentrations of 12.5, 25, 37.5 and 50 mM

caused an increase in the average diameter. The growth time of 3, 5, 7, and 9 h showed a remarkable increase in the average diameter of the NRs, with an increase in the length until 7 h; however, increase the growth time to 9 h caused a decrease in the length. The growth temperatures of 65, 75, 85 and 95 ^{o}C showed a noticeable increase in both the average diameter and length of NRs. The average diameter increased to 160 nm from 70 nm and the length increased to 4300 nm from 400 nm.

Poornajar et al. [58] studied the effects of physicochemical factors on properties of ZnO NRs prepared in glass substrates using the CBD technique. They that the found as-grown NRs were affected by the growth parameters, such as the growth temperature and concentration of initial Zn ions. Increase the growth temperature from 80 to 85 ^{o}C caused an increase in the NRs length by four times, with an increase in the average diameter as well. However, increasing the temperature to 90 ^{o}C caused a reduction in the NRs length. The decrease in length for NRs at high temperature could be attributed to the reduction in NH_3 solubility and OH^{-1} concentration, which reduces the growth of ZnO. The sample prepared using Zn ion concentration of 25 mM showed the highest aspect ratio. However, increasing the concentration to 50 mM reduces the ratio due to the decrease in length of NRs. The decrease in the length of NRs at high concentration referred to the nucleation of some of Zn^{+2} and OH^{-1} in the solution instead of setting in typical sites in the lattice.

Kim et al. [67] prepared ZnO NRs using the hydrothermal method. They found that the growth time played an important role in the morphology properties of ZnO. They demonstrated that the NRs aspect ratio is directly dependent on the growth time. Bao et al. [65] prepared NSs by the hydrothermal method. They found that the HMTM concentration had significant effects on the morphology, structure and optical properties of ZnO. They found that low HMTM concentration produces

the rod-like shape. However, at high HMTM concentration the ZnO nanoflowers have been grown. It was suggested that HMTM attaches to the nonpolar surfaces of ZnO i.e. (002), which inhibits the growth into this direction that generates nanoflowers.

Farhat et al. [57] studied the effects of substrate types on the properties of ZnO NRs prepared using CBD method. They reported that the NRs grown on a Si substrate had better quality than that grown on glass and PET (polyethylene terephthalate) substrates. This could be due to the low lattice and thermal mismatches between ZnO and Si substrate compared with lattice and thermal mismatches between ZnO and PET and glass substrates.

Recently, Chee et al. [68] studied the effects of precursor concentration and growth temperature on the properties of ZnO NRs prepared on FTO (F-doped SnO_2) substrate using the hydrothermal technique. They demonstrated that the structure and optical properties of the prepared NSs were strongly influenced by the grown conditions such as the growth temperature and concentration of initial Zn ions.

2.5 Doping in semiconductors

Doping is the addition of small amounts of impurities into an intrinsic semiconductor, which leads to a change in the properties of the hostel material [69]. The added impurities can change the morphological, structural, optical, and electrical properties of the intrinsic semiconductor [5, 70, 71].

Two types of doping can be classified: the n-type and p-type, as illustrated in Figure 2.3. For the n-type, the added element has valence electrons more than that of the substituted element. Therefore, it can provide the host material by extra free electrons. In this case, the impurity atoms create shallow donor levels below the

conduction band (CB); these atoms provide CB by freeing electrons that lead to the enhancement of the electrical properties and other related properties such as optical properties and energy band gap. Another type of doping is the p-type; in this case, the added element tries to gain electrons from the host material because it has valence electrons less than that of the substituted element. The impurity atoms create acceptor levels above the valence band (VB); these atoms can accept electrons from VB [1].

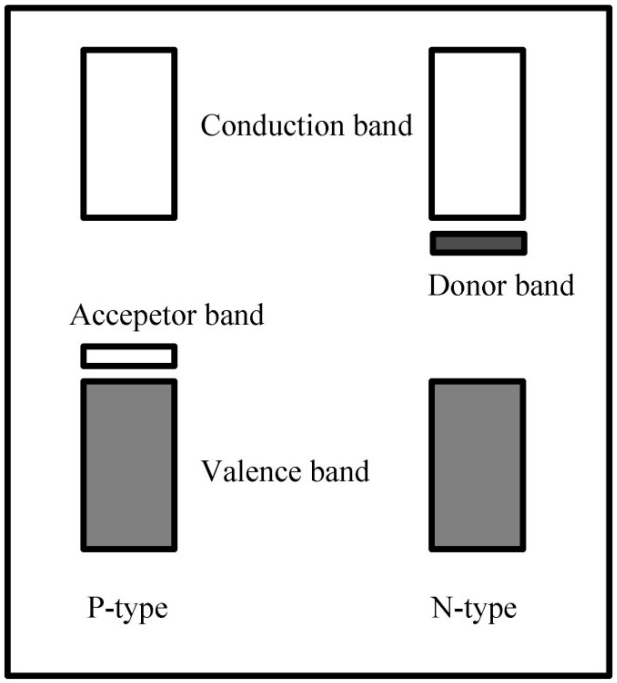

Figure 2-3 Types of doping in ZnO semiconductor [72].

2.6 Ti-doped ZnO

2.6.1 TiO_2 as a Ti source

Titanium dioxide (TiO_2) is an important n-type semiconductor material with promising properties such as chemical stability, low cost, non-toxicity and photo-catalytic activity [73-75]. TiO_2 have been used in various potential applications such as a white pigment in industrial fields, including paints and paper manufacturing. It's

also employed in pharmaceutical applications; TiO_2 is used as a tablet coating [76]. In addition, TiO_2 NSs have potential applications such as gas sensors, dye-sensitised solar cells, UV detectors and photovoltaic devices [73, 77, 78]. TiO_2 was extensively used to prepare Ti-doped ZnO using physical methods. However, TiO_2 has not been reported to synthesise Ti-doped ZnO NSs using non-physical (chemical). Therefore, this work attempted to provide better insight in this area which could lead to further researches and novel potential applications.

2.6.2 Effects of ultrasonic treatment

Ultrasound waves involve a series of compression and rarefaction waves; it can affect the chemical and physical properties of the molecules in the medium which it propagates in [79]. The influence of ultrasonic waves is referred to the acoustic cavitation effect. When ultrasound waves propagate in a liquid medium, the cavitation bubbles are generated; these bubbles vibrate many times and their size increase, leading to collapse [80]. The collapse of the bubbles is accompanied by the generation of extraordinary values of pressure and temperature that reach to 1000 atm and 5000 K [34]. These conditions can rupture chemical bonds and increase the dissolving of solids into liquids [33]. This ambient has a vital role in dissociating TiO_2 molecules, thereby, favouring the dissolution of Ti within the ZnO host lattice.

Recently, ultrasonic waves have been used to break TiO_2 powder. It was reported that ultrasonic waves play a crucial role in the breakdown of powder materials, hence could be used to break the bonds between the particles [81].

2.6.3 Effects of Ti on properties of ZnO

Introduction of Ti into the ZnO NSs could modify its physical properties such as morphological, structural, electrical, and optical properties. This section

summarises effects of Ti on the ZnO properties. Through the growth process of CBD technique, Zn^{+2} and O^{-2} try to arrange themselves in the proper sites of the lattice structure (the proper site means the typical site in a lattice structure). By adding Ti into the deposition pot, it has a chance to incorporate into the lattice structure. Ti^{+4} has a smaller ionic size compared to Zn^{+2} (0.068/0.074). Therefore, it can easily replace Zn^{+2} ions at substitutional sites without a notable change in the ZnO lattice structure. Furthermore, it can occupy the interstitial space within the lattice [22, 28]. Figure 2.4 explains the incorporation of Ti ions in ZnO lattice. It can be observed that the Ti ion can substitute Zn site without changes in the original lattice structure because of the small ionic size in Ti ion compared with the ionic size of Zn ion. In addition, Ti can occupy the interstitial space as interstitial point defect.

Doping in semiconductor causes changes in the lattice parameters [82]. The incorporation of Ti into the ZnO lattice structure affects the lattice parameters due to various reasons such as the difference in the radii between the host and dopant ions and the presence of Ti in the interstitial space [83].

Substitution of Ti into the Zn^{+2} sites in the ZnO lattice structure supports the lattice by freeing extra electrons that increase the carrier concentration. These electrons can move into CB, as a result, increasing the conductivity and then reducing the resistivity. In addition, this leads to an enhancement in the electrons' mobility. This behaviour indicates that the doping with high valence electrons compared to the substituted cation can modify the electrical properties that are useful for different applications [25, 84].

The optical properties are affected by doping. The generated electrons due to the substitution of Ti into the Zn sites can move into CB and fill in the lowest energy states. This causes a widening of the band gap, which then increases the

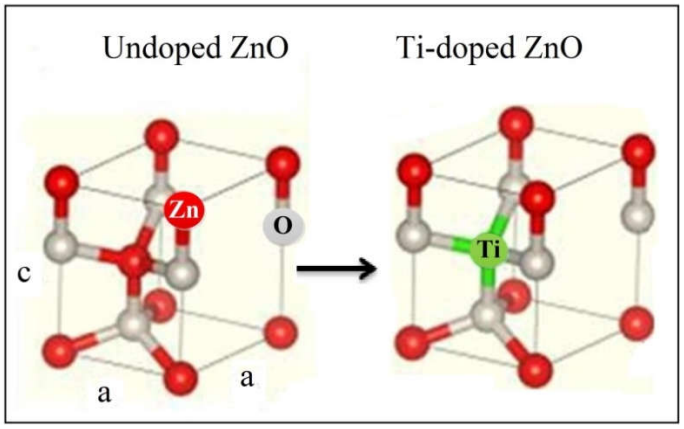

Figure 2-4 Schematic diagram explains the incorporation of Ti in ZnO lattice structure [83].

energy band gap (E_g) belonging to the Burstein Moss (BM) effect [71]. Figure 2.5 shows how doping can modify the band gap of the semiconductor [85], where ΔE is the increment of E_g due to increasing in the carrier concentration. Ti-doped ZnO NSs showed an increase in E_g, which could be useful for applications that depend on E_g such as UV photo-detection applications. In addition, the visible emission of ZnO is affected by defects and impurities. Ti-doped ZnO involves adding impurities and generating defects. Ti-like impurities enhance the visible emission in the Ti-doped ZnO NSs [15, 21, 25].

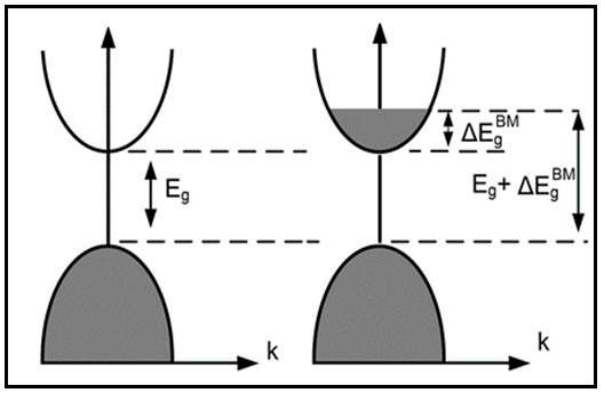

Figure 2-5 Schematic diagram of Burstein–Moss effect on the energy band gap [86].

2.7 Ti-doped ZnO NSs

This section presents previous works on Ti-doped ZnO NSs that were prepared using different physical and chemical techniques. The growth conditions that affect the properties of the as-grown structures are discussed. Ti sources and the procedures of doping process are also discussed.

2.7.1 Ti-doped ZnO prepared using physical techniques

An early work on Ti-doped ZnO NSs was reported by Gutman et al. [87]. In their study, ZnO thin film was coated with Ti atoms using thermal evaporation process for sensing applications. They found that the gas sensor based on Ti-doped ZnO had a better responsibility (two orders) in comparison to the undoped film. The responsibility of doped device is two orders high in comparison to the undoped device. Ti could improve the chemical activity of ZnO surface where Ti is a donor and can generate active-adsorption sites at the surface of NSs and then enhances the responsivity.

Park and Kim [88] prepared Ti-doped ZnO thin films by RF magnetron sputtering on Al_2O_3 substrates. They studied the effects of substrate temperature on the physical properties of the as-grown films. They concluded that increasing the substrate temperature caused an increase in the Ti composition in the doped film, and this led to an increase in Ti-related defects. These defects are generated when Ti-doped atoms substitute Zn sites and occupy the interstitial space within the lattice structure. The XRD results of the doped films showed a degradation on the structural quality; this was attributed to the presence of the Ti-related defects. These defects also caused an increase in the lattice constant in the *c*-direction of the Ti-doped ZnO film compared to the undoped ZnO structure.

Chen et al. [16] prepared Ti-doped ZnO thin films using a magnetron RF-sputtering system. They reported that Ti atoms can substitute the zinc atomic sites in the hexagonal lattice structure. The fact that Ti has balance electron of 4 while Zn has balance electrons of 2, the substitution process generates 2 free electrons, and therefore, increases the free carrier concentration. These electrons can migrate to CB and fill in the lowest energy levels, which causes an increase in E_g that refers to the BM effect. In addition, Ti-doped ZnO NSs were reported by different research groups using various physical methods such as atomic laser deposition [20], solid state reaction [21], pulsed laser deposition [22], furnace system with hotwire assistance [15], and cathode arc-plasma method [89].

2.7.2 Ti-doped ZnO prepared using chemical techniques

The non-physical methods, including chemical techniques, were also reported to synthesise Ti-doped ZnO NSs. Shewale and Yu [25] reported the synthesis of Ti-doped ZnO thin films by chemical spray pyrolysis method on glass substrates using zinc acetate ($C_4H_6O_4Zn{\cdot}2H_2O$) and titanyl acetylacetonate ($TiC_{10}H_{14}O_5$). The effects of Ti on structural, morphological, optical and gas sensing properties were investigated. The PL results demonstrated a strong enhancement in the visible emission of the doped samples; this was attributed to Ti impurities. The sensing responsibility had improved by 152.63% after using Ti; this was referred due to the generation of active adsorption sites on the surface of the as-grown film.

Yilmaz and Turgut [26] deposited Ti-doped ZnO thin films on glass substrates by spin coating sol-gel method using zinc acetate dehydrate ($C_4H_6O_4Zn{\cdot}2H_2O$) and titanium (IV) butoxide ($C_{16}H_{36}O_4Ti$). They found that the morphology changed from nanoparticles for the undoped ZnO to nano network for the Ti-doped

samples. The crystalline quality of doped samples was degraded in comparison with the undoped sample. This represents the presence of Ti like impurities in doped samples. The energy band gap increased at the concentration of 1% of dopant material; however, it decreased at further concentrations.

Tseng et al. [29] investigated the effects of Ti incorporation on optical and structural properties of ZnO nanoparticles that prepared by the sol–gel method using titanium (IV) isopropoxide ($C_{12}H_{28}O_4Ti$) and zinc acetate dehydrate $C_4H_6O4Zn\cdot 2H_2O$. The PL results showed an enhancement in UV emission intensity with quenched in green emission intensity. They attributed that to a decrease in a number of oxygen vacancies. XRD results revealed a decrease in X-ray diffraction peaks' intensities with increasing Ti, which indicated to reduce in the crystalline structure of the doped films. Raman shift of the doped sample exhibited a decrease in $E_2(H)$ peak intensity with quenched of the $E_1(L)$ compared to the undoped sample. Since $E_2(H)$ represents a typical Raman peak of hexagonal ZnO wurtzite structure [45]; therefore, this decrement indicated a reduction in the crystalline quality as revealed by XRD results.

Güntner et al. [83] prepared Ti-doped ZnO nanoparticles by flame spray pyrolysis technique using titanium (IV) isopropoxide ($C_{12}H_{28}O_4Ti$) and zinc 2-ethylhexanoate ($C_{16}H_{30}O_4Zn$). They found that the lattice constants expanded after using Ti. They attributed this behaviour to the substitution of Ti^{4+} into the hexagonal lattice, as well as to the repulsive force between Ti^{+4} and Zn^{+2} due to the difference in their charges. They reported that the crystallite size had reduced after using Ti from 19 nm for undoped ZnO to 16 nm for Ti-doped ZnO. They attributed the decrement in the crystallite size to the incorporation of Ti^{+4} as defect points in the lattice structure during the growth process.

Liu et al. [27] deposited Ti-doped ZnO NRs by the hydrothermal method and a polystyrene nano-sphere monolayer mask using TBOT (tetrabutyl-orthotitanate, $C_{16}H_{36}O_4Ti$) and zinc nitrate hexahydate (($Zn(NO_3)_2.6H_2O$) on silicon substrates. They reported that the UV emission peak of the doped samples was blue-shifted with the increase of the Ti doping content, which indicated an increase in the energy band gap. Carrier of concentration also increased with the increasing Ti due to substitute Ti into Zn site. The visible emission was also strongly enhanced due to the increase in defects after doping.

Lately, Lv et al. [28] prepared Ti-doped ZnO NRs using the facile ultrasonic irradiation-assisted alcohol-thermal method. ZnO colloids were prepared using zinc acetate dihydrate ($Zn(Ac)_2.2H_2O$), and the Ti solution was prepared using TBOT. They reported that incorporation of Ti into ZnO structure caused degradation in the crystalline quality and a decrease in the intensities of NBE and DLE. This degradation could refer to gather the dopant atoms on the surface of the grain boundary of the lattice that generates the grain boundary defects.

Kanmani et al. [30] prepared the Ti-doped ZnO chunk-shaped NSs using CBD method. They employed titanium (IV) isopropoxide and zinc acetate dihydrate as the Ti and Zn sources, respectively. They concluded that Ti atoms could substitute the Zn site or stay in an interstitial space within the ZnO crystal lattice. They found that the lattice constant was increased after Ti doping and the crystalline quality of doped films was reduced; they referred this degradation to the incorporation of Ti atoms within the ZnO lattice structures. The XRD pattern showed an independent TiO_2 phase that was noticed at 5 moles % of Ti precursor. The energy band gap was reduced with the increase in the Ti content.

Hsu et al. [90] reported the growth of Ti-doped ZnO NSs using CBD. They used ($C_4H_6O_4Zn.2H_2O$) and ($C_{12}H_{28}O_4Ti$) as Zn and Ti sources, respectively. They found that XRD results showed a low crystalline structure of Ti-doped ZnO NSs, this referred to Ti like impurities that can degrade the crystalline quality. Accumulating the dopant atoms on the surface of the grain boundary of the lattice generates the grain boundary defects that degrade the crystalline quality. Table 2.2 summarizes previous works on Ti-doped ZnO NSs that have been prepared using different chemical methods.

Table 2-2 Previous works have been reported on Ti-doped ZnO NSs using different chemical methods.

Method	**Ti source**	**Structure**	**References**
Sol-gel	Titanium (IV) butoxide $C_{16}H_{36}O_4Ti$	Nano-network	[26]
	Tetrabutyl titanate $C_{16}H_{40}O_4Ti$	Thin film	[91]
	Titanium (IV) isopropoxide $C_{12}H_{28}O_4Ti$	Nanoparticles	[29]
Spry pyrolysis	Titanyl acetylacetonate $TiC_{10}H_{14}O_5$	Thin film	[25]
	Titanium (IV) isopropoxide $C_{12}H_{28}O_4Ti$	Nanoparticles	[83]
Electrochemical deposition	Ammonium-hexafluoroti-tanate $(NH_4)_2TiF_6$	Thin film	[31]
Hydrothermal method	TBOT (Tetrabutyl orthotitanate) $C_{16}H_{36}O_4Ti$	NRs	[27, 28]
Chemical bath deposition	Titanium (IV) isopropoxide. $C_{12}H_{28}O_4Ti$	Chunk-shaped nanostructure	[30]
		Thin film	[90]

2.8 MSM UV-photodetectors

2.8.1 General background

The photodetector (PD) is an optoelectronic application that absorbs the optical radiation and converts it to the electrical signals in photo-current form. UV-PDs have gained a high interest in scientific research and industrial applications. This application is employed in various fields such as flame detection, space communications, solar UV monitoring and, finally, in chemical and biological sensors (ozone detection and monitoring of pollution levels in the air) [92-94].

To fabricate a PD, a metal-semiconductor contact is essential. The work' function that is defined as the minimum amount of energy needed to remove an electron from the surface of a metal is an important factor need to be considered. Two types of metal-semiconductor contacts can be employed; ohmic and Schottky contacts. In the case of ohmic contact, the metal has a lower work function than that of the semiconductor (n-type), and the metal–semiconductor junctions obeys Ohm's law with a linear relation of I-V curve. For Schottky contact, the work function of the metal is more than that of the semiconductor. In this case, the I-V curve has a rectifying behaviour. The electrons (current) across the metal-semiconductor show a non-linear behaviour. When the electrons move from CB of the semiconductor to the metal contact, a negative charging layer called depletion layer is generated. The electrons movement generates an electric field that results in a built-in-potential. This potential near to the metal-semiconductor interface. The generated potential bends the band gap of the semiconductor near the metal interface as well. In the equilibrium state, the potential can control the electrons' movement in both directions; from the metal to the semiconductor and vice versa [95].

When an n-type semiconductor is connected to metal contact of higher work function a depletion layer near to the contact interface is generated. More so, as the metal and semiconductor are connected to the positive and negative terminals of a battery respectively, the depletion layer is reduced. This will increase the electrons flow rate (current) from CB of the semiconductor to the metal interface and thus, a notable current is obtained. However, when the connection is reversed, that is metal to the negative terminal and semiconductor to the positive terminal the depletion layer is increased. In this case the electrons flow rate (current) is reduced, and a small current is usually obtained [95]. In this study, Schottky metal contact was used to fabricate MSM-photo-detectors. Figures 2.6 shows a schematic diagram of this type of contact.

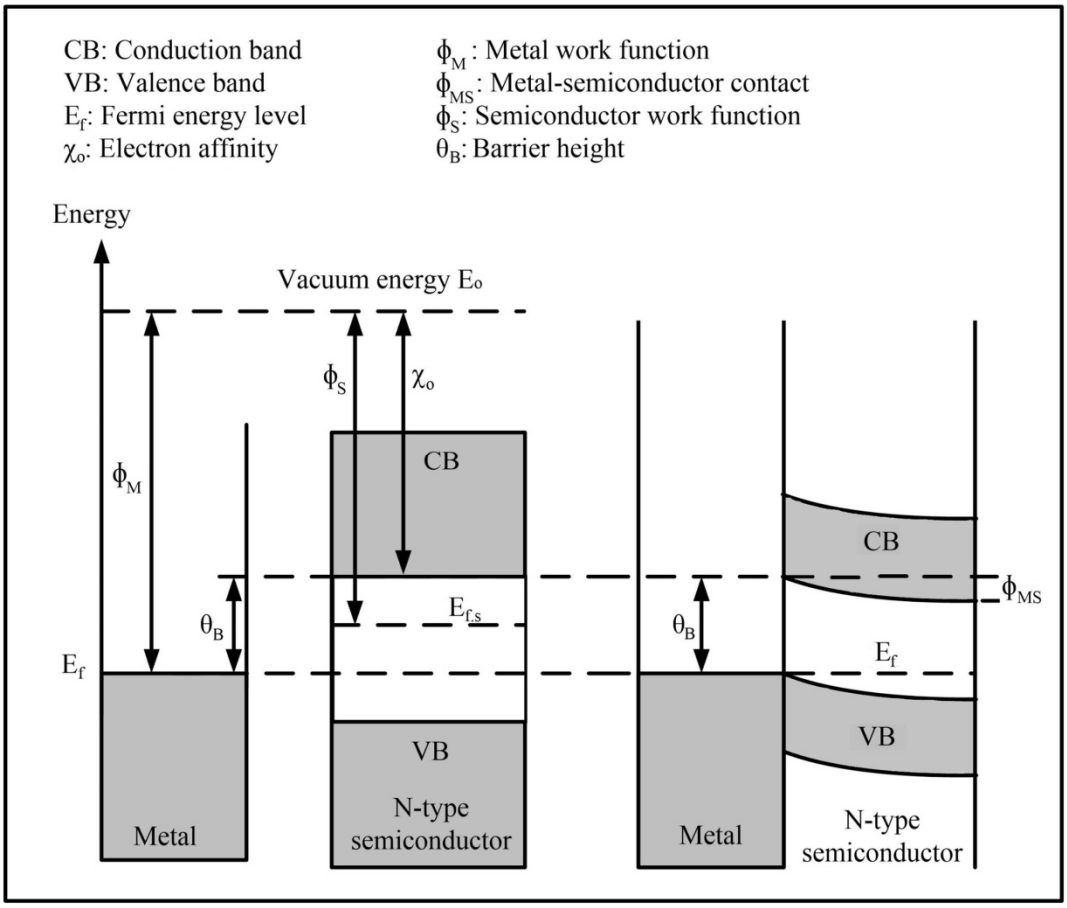

Figure 2-6 Schematic diagram of Schottky metal contact that used to fabricate MSM-photodetector [96].

The photodetector device possesses various parameters that characterise the quality of the device. These parameters include responsivity (R), sensitivity (S), current gain (G) and rise and fall times.

The responsivity (R) is defined as the ratio of the photocurrent (I_{ph}) to the optical power (P) of the light source. R can be expressed as follows [7]:

$$R = \frac{I_{ph} - I_d}{P} \tag{2.6}$$

The sensitivity (S) of a PD is defined as the ratio of the photocurrent to the dark current (I_d).

$$S = \frac{I_{ph} - I_d}{I_d} \times 100\% \tag{2.7}$$

The current gain (G) is defined as the ratio of the photocurrent (I_{ph}) to the dark current (I_d). G can be expressed as follows [62]:

$$G = \frac{I_{ph}}{I_d} \tag{2.8}$$

The rise time is the time that the photocurrent needs to increase from 10% to 90% of its saturation value, whereas the fall time is the time that the photocurrent needs to drop from 90% to 10% of its saturation value [77].

2.8.2 Theoretical mechanism of photoconduction in ZnO

The photoconduction in n-type ZnO results from the adsorption and desorption of oxygen molecules on the surface of the NRs. That leads to a change in the electrical conductivity. In the dark, the oxygen molecules are adsorbed onto the surface of the ZnO NRs; then they capture the free electrons from the ZnO which reduces the concentration carrier and then the conductivity, generating a low dark